Controlling the wave propagation through the medium designed by linear coordinate transformation

2015 Eur. J. Phys. 36 015006

(http://iopscience.iop.org/0143-0807/36/1/015006)

IOP Publishing European Journal of Physics
Eur. J. Phys. **36** (2015) 015006 (11pp) doi:10.1088/0143-0807/36/1/015006

Controlling the wave propagation through the medium designed by linear coordinate transformation

Yicheng Wu, Chengdong He, Yuzhuo Wang, Xuan Liu and Jing Zhou

Applied Optics Beijing Area Major Laboratory, Department of Physics, Beijing Normal University, Beijing 100875, People's Republic of China

E-mail: jzhou@bnu.edu.cn

Received 26 June 2014, revised 9 September 2014
Accepted for publication 16 September 2014
Published 6 November 2014

Abstract

Based on the principle of transformation optics, we propose to control the wave propagating direction through the homogenous anisotropic medium designed by linear coordinate transformation. The material parameters of the medium are derived from the linear coordinate transformation applied. Keeping the space area unchanged during the linear transformation, the polarization-dependent wave control through a non-magnetic homogeneous medium can be realized. Beam benders, polarization splitter, and object illusion devices are designed, which have application prospects in micro-optics and nano-optics. The simulation results demonstrate the feasibilities and the flexibilities of the method and the properties of these devices. Design details and full-wave simulation results are provided. The work in this paper comprehensively applies the fundamental theories of electromagnetism and mathematics. The method of obtaining a new solution of the Maxwell equations in a medium from a vacuum plane wave solution and a linear coordinate transformation is introduced. These have a pedagogical value and are methodologically and motivationally appropriate for physics students and teachers at the undergraduate and graduate levels.

Keywords: wave control, transformation optics, maxwell equations, linear coordinate transformation

1. Introduction

In traditional wave optics, optical design is largely a matter of choosing the interface between two materials. For example, the lens of a camera is optimized by altering its shape so as to

minimize geometrical aberrations. Based on the form invariance of Maxwell equations under spatial transformation, transformation optics (TO) provides a powerful mathematical technique for designing electromagnetic wave control devices. Different from a traditional approach, in TO, a new solution of the Maxwell equations in a medium could be obtained from a vacuum plane wave solution and a coordinate transformation, and the material parameters of the medium could be derived from the coordinate transformation applied. Extensive attention was paid to this unique method beginning with two papers published back to back in *Science* written by Pendry *et al* [1] and Leonhardt [2], which were aimed at realizing the electromagnetic/optical cloak of invisibility. Now supported by the advent of metamaterials, TO offers great flexibility for controlling electromagnetic waves [3, 4]. Various devices have been designed, including the invisibility cloak [3–14], wave collimators [15–17], beam bender [16, 18] and beam compressors/expanders [18], hyperlens [11, 19], polarization splitter [20, 21], optical illusion device [3], etc. Nevertheless, most devices require an inhomogeneous anisotropic medium with material parameters of very large values or even infinities. This is difficult to realize in practical application. In this paper, we propose to design a wave control device with a homogeneous anisotropic medium using linear transformation. The values of the material parameters are small. As examples, the beam bender, polarization splitter, and illusion device are designed.

The conception and the analysis method introduced or proposed in this paper are new and comprehensively apply the fundamental theories of electromagnetism and mathematics. These have a pedagogical value and are methodologically and motivationally appropriate for physics students and teachers at the undergraduate and graduate levels.

2. The principle of design

In transformation optics, the coordinate transformation is equivalent to the changes of the permittivity and permeability of the medium, and the new solution of the Maxwell equations in the medium could be obtained from a vacuum plane wave solution and the coordinate transformation applied. This provides a unique method to control the material properties and could enable a powerful form of electromagnetic design [2]. Exhaustive description about the relation of the coordinate transformation and the electromagnetic properties of the material could be found in [2, 22]. Here we give a brief explanation.

A transformation from the original coordinate system (x_1, x_2, x_3) to the transformed coordinate system (x_1', x_2', x_3') could be represented by the coordinate transformation functions

$$x_1' = x_1'(x_1, x_2, x_3), \quad x_2' = x_2'(x_1, x_2, x_3), \quad x_3' = x_3'(x_1, x_2, x_3). \quad (1)$$

(x_1', x_2', x_3') represents the location of the new point with respect to the x, y, and z axes. Lines of constant x_i', x_j' define the generalized x_k' axis, with $i, j, k = 1, 2, 3$ and $i \neq j \neq k$. Thus, a set of points with equal increments along the x_1', x_2', x_3' axes might form a distorted mesh. Obviously, the shape of the distorted mesh is closely related to the coordinate transformation functions. Two distorted meshes realized by different coordinate transformations are presented in figure 1. As shown by the red lines, straight lines in the original system might be changed to curved lines.

According to the form invariance of Maxwell equations under spatial transformation, all of the Maxwell equations should have exactly the same form in any coordinate system, while the permittivity and permeability should be scaled by a factor; or the permittivity and permeability in the transformed coordinate system should be renormalized [2]. We note these

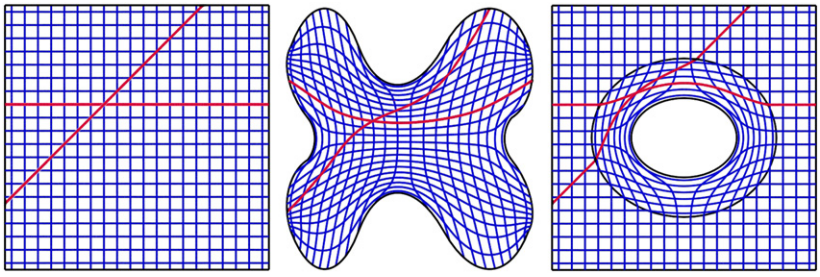

Figure 1. Schematic demonstration of the space distortion caused by coordinate transformation. (a) Simple cubic lattice of points in the original uniform coordinate system. (b) Distorted mesh caused by an arbitrary coordinate transformation. (c) Coordinate mesh realized by transforming the central point of the original system to the inner elliptical boundary and keeping the outer elliptical boundary unchanged.

renormalized permittivity and permeability by ε' and μ'. For the conserved quantity of electromagnetism such as the Poynting vector $\vec{S}$, the straight field lines in the original system would be twisted in the transformed system with the renormalized material parameters of ε' and μ', as shown by the red lines in figure 1. This means that in the transformed material of ε' and μ', the conserved quantities of electromagnetism could be directed at will through proper coordinate transformation. For example, the transformation shown in figure 1(c) could be used to realize the cloaking of an arbitrary object contained in the central oval space; the external observers are unaware the existence of the object [2].

Considering a transformation from the original Cartesian coordinates (x, y, z) to the transformed coordinate system (x', y', z'), the forms of the Maxwell equations and the constitutive equations in the transformed system remain unchanged:

$$\nabla_{(x',y',z')} \times \vec{E}' - \mu_0\mu' \frac{\partial \vec{H}'}{\partial t} \tag{2a}$$

$$\nabla_{(x\prime,y\prime,z\prime)} \times \vec{H}' = -\varepsilon_0\varepsilon' \frac{\partial \vec{E}'}{\partial t} \tag{2b}$$

$$D' = \varepsilon_0\varepsilon' E', \quad B' = \mu_0\mu' H' \tag{2c}$$

with $\nabla_{(x',y',z')} = \frac{\partial}{\partial x'}\hat{e}_{x'} + \frac{\partial}{\partial y'}\hat{e}_{y'} + \frac{\partial}{\partial z'}\hat{e}_0$.

The general forms of ε' and μ' are tensors. Through strict mathematical derivation, it can be concluded that ε' and μ' could be calculated by the following formulas [22]:

$$\varepsilon' = \frac{A\varepsilon A^T}{\det(A)}, \quad \mu' = \frac{A\mu A^T}{\det(A)} \tag{3}$$

where, ε and μ are the permittivity and permeability in the Cartesian original coordinate system. The character A denotes the Jacobi matrix of the transformation, and $\det(A)$ represents the determinant of A. The elements of A are determined by the coordinate transformation functions

$$A_{ij} = \frac{\partial x_i'}{\partial x_j} \quad i, j = 1,2,3 \tag{4}$$

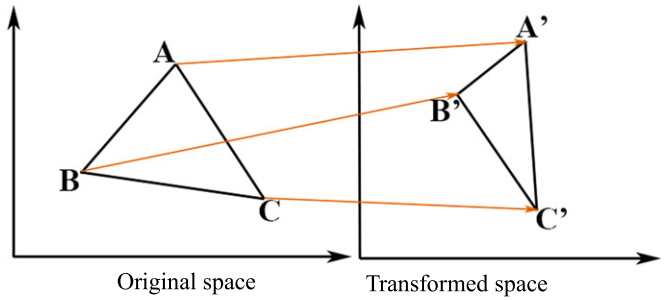

Figure 2. The scheme of the linear transformation realized through triangular areas.

For three-dimensional Cartesian coordinates, $(x_1, x_2, x_3) = (x, y, z)$, $(x'_1, x'_2, x'_3) = (x', y', z')$. The determinations of the elements of A are crucial. Several examples that clearly show the calculation of A can be found in [16, 20]. Obviously, the element A_{ij} will be constant and independent of x_i' when the transformation functions $x_i'(x_j)$ are linear. And then the permittivity and permeability of the transformed area ε' and μ' are independent of x_i' also. It is known that an n-dimensional linear transformation can be expressed as $x'_i(x_j) = \sum_{j=1}^{n} k_{ij}x_j + c_i$, where k_{ij} and c_i are coefficients independent of the space coordinates. For the two-dimensional case $n = 2$, the transformation can be written as

$$\begin{cases} x'(x, y) = k_{11}x + k_{12}y + c_1 \\ y'(x, y) = k_{21}x + k_{22}y + c_2 \\ z'(x, y, z) = z \end{cases} \tag{5}$$

Subsequently, the Jacobi matrix can be written as

$$A = \begin{pmatrix} k_{11} & k_{12} & 0 \\ k_{21} & k_{22} & 0 \\ 0 & 0 & 1 \end{pmatrix}, \tag{6}$$

and the material parameters can be calculated using equation (3)

$$\varepsilon' = \mu' = \begin{pmatrix} \left(k_{11}^2 + k_{12}^2\right)/\det(A) & \left(k_{11}k_{21}k + k_{12}k_{22}\right)/\det(A) & \\ \left(k_{11}k_{21} + k_{12}k_{22}\right)/\det(A) & \left(k_{21}^2 + k_{22}^2\right)/\det(A) & \\ & & 1/\det(A) \end{pmatrix} \tag{7}$$

The function $x_i' = x_i'(x_j)$ used for space transformation should satisfy two conditions. First, $x_i' = x_i'(x_j)$ does not produce a singular point. Second, the boundaries of the regions in the original and transformed spaces should be related by the function $x_i' = x_i'(x_j)$. It can be seen from equation (5) that there should be three independent transform relations to determine the coefficients. Therefore, three and only three points on the boundary of the transform region could be controlled, and it can be realized through the transformation of the triangular region. As shown in figure 2, three points A, B, C in the original space are transformed to A', B', C' in the transformed space. The triangular region ΔABC is transformed to $\Delta A'B'C'$.

Usually, the materials with the permeability and permittivity designed in this way cannot be a naturally existing material and can be made using newly developed metamaterials technology [3]. The main advantage of the device designed by such linear transformation is

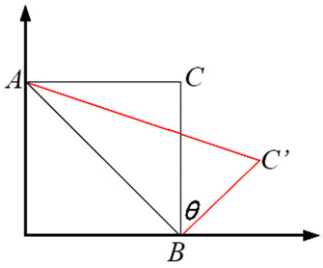

Figure 3. The space transformation for beam bender and polarization splitter. The area of the transformation region remains unchanged throughout the transformation.

that the material parameters are constants. Thus, the material is homogenous. And when the size of the device changes, the material parameters remain unchanged.

3. Beam bender and polarization splitter of non-magnetic homogenous materials

In this section, a linear transformation is proposed to bend the beam propagation direction, which can also be used to realize the polarization splitting. In order to achieve the design with a non-magnetic material, a special kind of linear transformation is used which could make the determinant of A have the value of one, or $\det(A) = 1$. In this case, it could be seen from equation (7) that the z components of the permeability and permittivity are units $\varepsilon_{zz} = \mu_{zz} = 1$. Such a transformation can be realized by keeping the area of the region unchanged as schematically shown in figure 3.

The isosceles right triangular region ΔABC is transformed into the triangular zone $\Delta ABC'$ by linear transformation. The areas of ΔABC and $\Delta ABC'$ are equal. The character θ represents the angle that the side $\overline{BC'}$ rotated from $\overline{BC}$. It can be derived from equation (5) that this transformation can be expressed as

$$\begin{pmatrix} x' \\ y' \\ z' \end{pmatrix} = \begin{pmatrix} k_{11} & k_{12} & 0 \\ k_{21} & k_{22} & 0 \\ 0 & 0 & 1 \end{pmatrix} \begin{pmatrix} x \\ y \\ z \end{pmatrix} + \begin{pmatrix} c_1 \\ c_2 \\ 0 \end{pmatrix}, \tag{8}$$

with

$$\begin{aligned} k_{11} &= \frac{1+2\tan(\theta)}{1+\tan(\theta)}, \quad k_{12}\frac{\tan(\theta)}{1+\tan(\theta)}, \quad c_1 = -\frac{\tan(\theta)}{1+\tan(\theta)}, \\ k_{21} &= -\frac{\tan(\theta)}{1+\tan(\theta)}, \quad k_{22} = \frac{1}{1+\tan(\theta)}, \quad c_2 = \frac{\tan(\theta)}{1+\tan(\theta)} \end{aligned} \tag{9}$$

Then according to equation (7), the material parameters of the transformed region could be formulated as

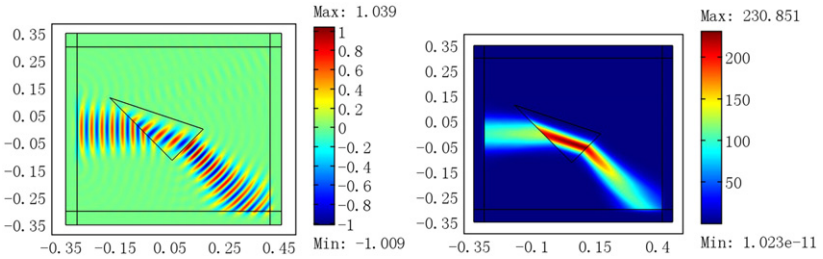

(a) H_z (b) $|S|$

Figure 4. The property of a 45° beam bender simulated by COMSOL Multiphysics. An 8 GHz Gaussian beam propagating along the x-axis is incident upon the device from the left. (a) Snapshot of the magnetic field distribution. (b) The magnitude distribution of the Poynting vector.

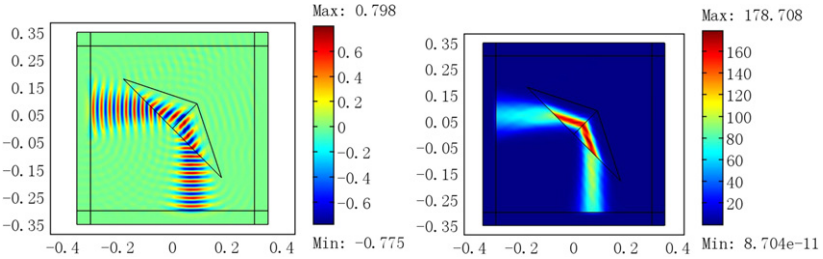

(a) H_z (b) $|S|$

Figure 5. Two connected 45° beam benders realize right-angle bending. (a) Snapshot of the magnetic field distribution. (b) The magnitude distribution of the Poynting vector.

$$\frac{\varepsilon'}{\varepsilon} = \frac{\mu'}{\mu} = \begin{pmatrix} \dfrac{5(\tan(\theta))^2 + 4\tan(\theta) + 1}{(\tan(\theta))^2 + 2\tan(\theta) + 1} & -2\dfrac{(\tan(\theta))^2}{(\tan(\theta))^2 + 2\tan(\theta) + 1} & 0 \\ -2\dfrac{(\tan(\theta))^2}{(\tan(\theta))^2 + 2\tan(\theta) + 1} & \dfrac{(\tan(\theta))^2 + 1}{(\tan(\theta))^2 + 2\tan(\theta) + 1} & 0 \\ 0 & 0 & 1 \end{pmatrix}. \tag{10}$$

Suppose $\varepsilon = \mu = 1$. In the original space, a beam propagating along the x axis and incident upon the region ΔABC from the left will emit from the side $\overline{BC}$ with no bending, while in the transformed space, the same wave incident upon the region $\Delta ABC'$ will emit from the side $\overline{BC'}$ propagating in the direction perpendicular to $\overline{BC'}$. Thus, the propagation direction of the beam will rotate by an angle of θ. The region $\Delta ABC'$ with the material parameters defined by equation (10) can be considered a beam bender. The performance of such a device can be numerically analyzed using a full-wave analysis tool based on the finite-element method (COMSOL Multiphysics). As an example, we set $\theta = 45°$, $\varepsilon = 1$, $\mu = 1$. It can be calculated that

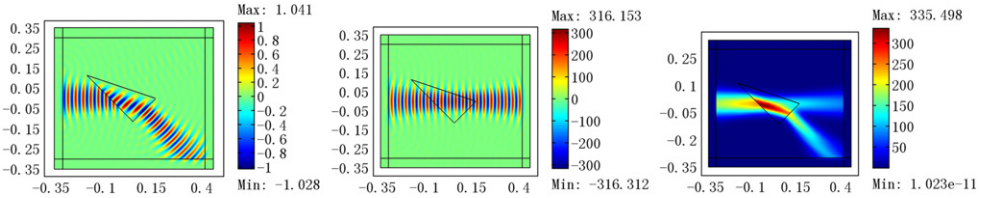

(a) H_z (b) E_z (c) $|S|$

Figure 6. The simulated results of the polarization splitter made of non-magnetic homogenous material. An 8 GHz circularly polarized Gaussian beam is incident upon the device from the left. (a) Snapshot of the field distribution of the *TM* wave H_z. (b) Snapshot of the field distribution of the *TE* wave E_z. (c) Magnitude distribution of the Poynting vector $|S|$.

$$\varepsilon' = \mu' = \begin{pmatrix} \frac{5}{2} & -\frac{1}{2} & 0 \\ -\frac{1}{2} & \frac{1}{2} & 0 \\ 0 & 0 & 1 \end{pmatrix}. \tag{11}$$

In the simulations without loss of generality, an 8 GHz Gaussian beam propagating along the x-axis is employed as the incident wave. The simulated result is shown in figure 4. Figure 4(a) is the snapshot of the magnetic field distribution, and figure 4(b) is the magnitude distribution of the Poynting vector. It can be seen that the propagation direction turned 45° when the beam passes through the device (or the transformed triangular $\Delta ABC'$).

The combination of several such beam benders can achieve large-angle bending. Figure 5 shows the simulated bending property of two connected 45° beam benders, which can rotate the propagation direction of the incident beam by 90°.

In the two-dimensional case, the transverse magnetic (TM) waves are affected only by μ_{zz}, ε_{xx}, ε_{xy}, ε_{yx}, and ε_{yy}, whereas the transverse electric (TE) waves interact only with ε_{zz}, μ_{xx}, μ_{xy}, μ_{yx}, and μ_{yy} [20]. The two sets of material parameters are completely independent of each other, and the behavior of transverse electric TE and TM waves can be controlled individually. If we set the parameters for the TM wave according to equation (10) and let the other parameters be same as the air, then a polarization splitter made of non-magnetic material can be obtained. Using $\theta = 45°$ as an example, the permeability and permittivity should be

$$\varepsilon' = \begin{pmatrix} \frac{5}{2} & -\frac{1}{2} & 0 \\ -\frac{1}{2} & \frac{1}{2} & 0 \\ 0 & 0 & 1 \end{pmatrix} \quad \mu' = \begin{pmatrix} 1 & 0 & 0 \\ 0 & 1 & 0 \\ 0 & 0 & 1 \end{pmatrix} \tag{12}$$

When a beam of arbitrary polarization is incident upon such a device, it will be separated into TM and TE waves, which will emerge propagating in different directions. Figure 6 shows the simulated results of such a polarization splitter. An 8 GHz circularly polarized Gaussian beam is incident upon the device from the left. Figures 5(a) and (b) are the snapshots of the field distributions for the TM wave (H_z) and TE wave (E_z), respectively. Figure 6(c) is the magnitude distribution of the Poynting vector $|S|$. It can be seen that the propagation direction of the TM wave rotated 45° and the TE wave propagated with no bending.

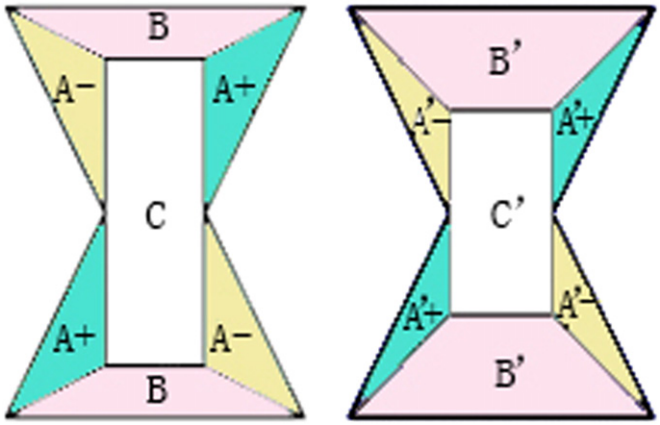

(a) The original space. (b) The transformed space.

Figure 7. The space transformation for realizing the magnification or compression of the object size.

4. Illusions

A transformation consisting of several triangular regions can realize the wave illusion. For example, the transformation for magnifying or compressing the subject size is shown in figure 7. The regions noted by $A+$, $A-$, B, and C in figure 7(a) are linearly transformed into the regions named $A'+$, $A'-$, B', and C' in figure 7(b), respectively. The ratio of the heights of C and C' is f, and the radio of the widths of C and C' is g. The transformation for $f>1$ ($g>1$) corresponds to the magnification in height (width), while $f<1$ ($g<1$) corresponds to the compression in height (width).

Take $f=1.5$, $g=1$ as an example. The material parameters of the regions $A'\pm$, B', C' can be calculated by equation (7) as follows:

$$\varepsilon'_{A\pm}=\mu'_{A\pm}=\begin{pmatrix}\frac{3}{2} & \pm 1 & 0\\ \pm 1 & \frac{4}{3} & 0\\ 0 & 0 & \frac{3}{2}\end{pmatrix}\quad \varepsilon'_{B}=\mu'_{B}=\begin{pmatrix}\frac{1}{2} & 0 & 0\\ 0 & 2 & 0\\ 0 & 0 & \frac{1}{2}\end{pmatrix}\quad \varepsilon'_{C}=\mu'_{C}=\begin{pmatrix}\frac{3}{2} & 0 & 0\\ 0 & \frac{2}{3} & 0\\ 0 & 0 & \frac{3}{2}\end{pmatrix}. \tag{13}$$

The values of all these parameters are small and constant, which illustrates that the material is homogenous. With these parameters, it can be expected that the object located in region C' will be viewed as an object with its height magnified by a factor of 1.5 for the observer outside the device. Figure 8 presents the simulation results. The incident beam is a plane wave propagating along the x-axis with the frequency of 8 GHz. Figure 8(a) is the electric field distribution scattered by a rectangular perfect electric conductor (PEC) object placed inside the region C'. Figure 8(b) shows the electric field distribution scattered by a rectangular PEC object placed in the free space, the height of which is enlarged to 1.5 times that of the PEC object in figure 8(a) and the width of which remains unchanged. It is shown that the field distributions in these two figures are completely the same for the outside viewers, which means that the height of the PEC object placed in region C' looks stretched by a factor of 1.5.

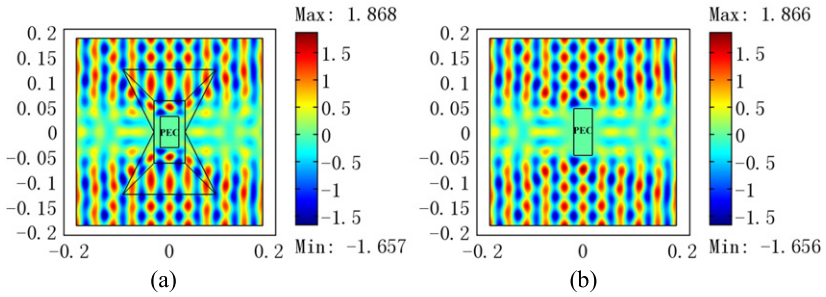

Figure 8. Simulated results for the magnification of the object size $f = 1.5$ and $g = 1$. (a) The electric field distribution scattered by a rectangular PEC object placed inside region C'. (b) The electric field distribution scattered by a rectangular PEC object placed in the free space, the height of which is 1.5 times that of the PEC object in figure 8(a) and the width of which remains unchanged.

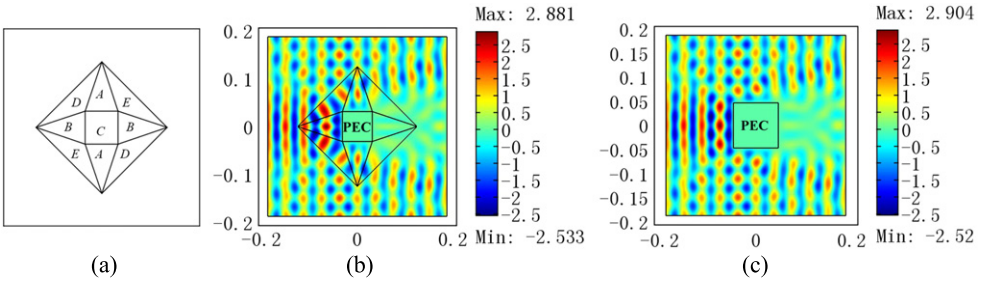

Figure 9. The magnification of object size with $f = 1.5$ and $g = 1.5$. (a) The transformation regions of the device. (b) The electric field distribution scattered by a square PEC object in region C. (c) The electric field distribution scattered by a square PEC object in the free space with the size 1.5 times that in (b).

Figure 9 is another example, with $f = g = 1.5$, which can realize the magnification of an object in x and y directions simultaneously. Figure 9(a) schematically shows the transformation regions. It can be worked out that the material parameters of the regions A, B, and C are diagonal tensors, $\varepsilon'_A = \mu'_A = \{5/9, 9/5, 5/4\}$, $\varepsilon'_B = \mu'_B = \{9/5, 5/9, 5/4\}$, and $\varepsilon'_C = \mu'_C = \{1, 1, 9/4\}$. And the parameters for the regions D and E are

$$\varepsilon'_D = \mu'_D = \begin{pmatrix} \frac{5}{4} & -\frac{3}{4} & 0 \\ -\frac{3}{4} & \frac{5}{4} & 0 \\ 0 & 0 & \frac{1}{2} \end{pmatrix} \quad \varepsilon'_E = \mu'_E = \begin{pmatrix} \frac{5}{4} & \frac{3}{4} & 0 \\ \frac{3}{4} & \frac{5}{4} & 0 \\ 0 & 0 & \frac{1}{2} \end{pmatrix}. \tag{14}$$

Still using an 8 GHz plane wave propagating along the x-axis as the incident wave, the simulated field distributions are presented in figure 9. It is shown that the square PEC object in region C looks like an object in the free space with the size magnified 1.5 times for the outside observers.

5. Conclusions

The method of controlling the wave propagation through the homogeneous anisotropic medium designed by linear coordinate transformation was proposed. Several devices, including a beam bender, polarization splitter, and illusion device, were designed as examples. The simulation results demonstrated the probability and the feasibility of the devices. The method is applicable to design other functional wave control devices as well. The conceptions and the analysis method introduced or proposed in this paper have a pedagogical value for students and teachers at the undergraduate and graduate levels.

Acknowledgement

The authors thank the National Natural Science Foundation of China (grant 61275130) and the National College Students′ Innovative Entrepreneurial Training Plan of China for financial support. The authors also thank Dr Jun Zheng and Prof Zhengming Sheng in Shanghai Jiaotong University for their help in numerical simulations.

References

[1] Leonhardt U 2006 Optical conformal mapping *Science* **312** 1777
[2] Pendry J B, Schurig D and Smith D R 2006 Controlling electromagnetic fields *Science* **312** 1780
[3] Chen H, Chan C T and Sheng P 2010 transformation optics and metamaterials *Nat. Mater.* 387–96
[4] Leonhardt U and Philbin T G 2006 General relativity in electrical engineering *New J. Phys.* **8** 247
[5] Schurig D, Mock J J, Justice B J, Cummer S A, Pendry J B, Starr A F and Smith D R 2006 Metamaterial electromagnetic cloak at microwave frequencies *Science* **314** 977
[6] Cai W, Chettiar U K, Kildishev A V and Shalaev V M 2007 Optical cloaking with metamaterials *Nat. Photon.* **1** 224
[7] Ruan Z, Yan M, Neff C W and Qiu M 2007 Ideal cylindrical cloak: perfect but sensitive to tiny perturbations *Phys. Rev. Lett.* **99** 113903
[8] Yan M, Ruan Z and Qiu M 2007 Cylindrical invisibility cloak with simplified material parameters is inherently visible *Phys. Rev. Lett.* **99** 233901
[9] Chen H, Wu B I, hang B and JA K 2007 Electromagnetic wave interactions with a metamaterial cloak *Phys. Rev. Lett.* **99** 063903
[10] Lai Y, Chen H, Zhang Z Q and Chan C T 2009 Complementary media invisibility cloak that cloaks objects at a distance outside the cloaking shell *Phys. Rev. Lett.* **102** 093901
[11] Gaillot D P, Croenne C, Zhang F and Lippens D 2008 Transformation optics for the full dielectric electromagnetic cloak and metal–dielectric planar hyperlens *New J. Phys.* **10** 115039
[12] Landy N and Smith D R 2013 A full-parameter unidirectional metamaterial cloak for microwaves *Nat. Mater.* **12** 25
[13] Luo Y, Zhang J, Chen H, Ran L, Wu B and Kong J 2009 A rigorous analysis of plane-transformed invisibility cloaks *IEEE Trans. Antennas Propag.* **57** 3926
[14] Chen X, Luo Y, Zhang J, Jiang K, Pendry J B and Zhang S 2011 Macroscopic invisibility cloaking of visible light *Nat. Commun.* **2** 1
[15] Jiang W X, Cui T J, Ma H F, Zhou X Y and Cheng Q 2008 Cylindrical-to-plane-wave conversion via embedded coordinate transformation *Appl. Phys. Lett.* **92** 261903
[16] Kwon D H and Werner D H 2008 Transformation optical designs for wave collimators, flat lenses and right-angle bends *New J. Phys.* **10** 115023
[17] Kwon D H and Werner D H 2009 Flat focusing lens designs having minimized reflection based on coordinate transformation techniques *Opt. Express* **17** 7807
[18] Rahm M, Roberts D A, Pendry J B and Smith D R 2008 Transformation optical design of adaptive beam bends and beam expanders *Opt. Express* **16** 11555
[19] Kildishev A V and Narimanov E E 2007 Impedance-matched hyperlens *Opt. Lett.* **32** 3432
[20] Kwon D H and Werner D H 2008 Polarization splitter and polarization rotator designs based on transformation optics *Opt. Express* **16** 1873110

[21] Zhai T, Ying Z, Jing Z and Liu D 2009 Polarization controller based on embedded optical transformation *Opt. Express* **17** 17206
[22] Leonhardt U and Philbin T G 2009 Transformation optics and the geometry of light *Prog. Opt.* **53** 69